Liang, Xingyuan et al.

Article

The effect of combined proppants upon the fracture conductivity in tight gas reservoirs

Energy Reports

Provided in Cooperation with:
Elsevier

Suggested Citation: Liang, Xingyuan et al. (2020) : The effect of combined proppants upon the fracture conductivity in tight gas reservoirs, Energy Reports, ISSN 2352-4847, Elsevier, Amsterdam, Vol. 6, pp. 879-884, https://doi.org/10.1016/j.egyr.2020.04.007

This Version is available at:
https://hdl.handle.net/10419/244085

Energy Reports 6 (2020) 879–884

Contents lists available at ScienceDirect

Energy Reports

journal homepage: www.elsevier.com/locate/egyr

Research paper

The effect of combined proppants upon the fracture conductivity in tight gas reservoirs

Xingyuan Liang, Fujian Zhou *, Tianbo Liang *, Yixiao Huang, Dongya Wei, Shiying Ma

State Key Laboratory of Petroleum Resources and Prospecting, China University of Petroleum (Beijing), Beijing 102249, China

ARTICLE INFO

Article history:
Received 29 January 2020
Received in revised form 23 March 2020
Accepted 3 April 2020
Available online xxxx

Keywords:
Fracture conductivity
Mixed proppant
Effective closure stress
Hydraulic fracture

ABSTRACT

Sand and ceramic proppant are the most commonly used materials to keep fractures open during hydraulic fracturing. Ceramic proppant has higher hardness and sphericity than sand, but it is much more expensive. To reduce the cost, sands are pumped at the beginning to replace a portion of ceramic proppants, while ceramic proppants are pumped at the end to support the fracture outlet where the effective closure stress is large. However, the effective conductivity of the propped fracture varies with the ratio of these two types of proppants, and it is worthy of laboratory investigation to determine the optimal substitution ratio of sands for fields with different effective closure stresses. In this work, the fracture conductivity with various ratios of sands to ceramic proppants is evaluated by an API standard Fracture Conductivity Evaluation System (FCS-842) under different effective closure stresses. Experimental results show that the fracture conductivity of the propped fracture decreases with the effective closure stress due to the crushing of proppants, while the decreasing rate of fracture conductivity is proportional to the ratio of sands to ceramic proppants within the propped fracture. Two empirical models are further derived from the results, which can be used to forecast the performance of fracture conductivity at different effective closure stresses and sand ratios. The findings of this work can guide people to optimize the sand ratio in the slurry when hydraulically fracturing the reservoirs at different depths with different effective closure stresses.

1. Introduction

The development of low-permeability reservoirs has drawn a great deal of attention in recent years. To obtain an economic production rate from such a reservoir, hydraulic fracturing needs to be applied to create a fracture network to maximize the drainage area of the reservoir (Liang et al., 2018; Merey, 2019). During hydraulic fracturing, proppants are pumped with the fracturing fluid to keep the created fractures open, and the conductivities of these propped fractures eventually determine the productivity of the well (Mittal et al., 2018; Zoveidavianpoor et al., 2018).

Sand and ceramic proppant are two major types of proppants applied in the field. Comparing to the sand, ceramic proppant has higher hardness and sphericity, both ensures a large fracture conductivity especially at high effective closure stress (Zhang et al., 2017). However, ceramic proppants are typically 3—5 times more expensive than sands, and they have larger densities that are unfavorable for the proppant transportation within the hydraulic fractures (Maity and Ciezobka, 2019). In a relatively low oil price environment, sands, especially the local sands, are suggested to be applied to substitute ceramic proppants despite their relatively poor performance on providing fracture conductivity. During hydraulic fracturing, sands are pumped during the pad injection and/or the beginning of slurry injection, which allows the proppants to travel far along the created fractures; then, ceramic proppants are pumped at the end of slurry injection, which supports the outlet where the fracture widths are large and thus the effective closure stress (Lei et al., 2005). However, since the hardness of proppants determines their crushing rates under different effective closure stresses, the effective conductivity of the propped hydraulic fracture varies with the ratio of sands to ceramic proppants. It is worthy of laboratory investigation to optimize the sand ratio in the slurry when hydraulically fracturing the reservoirs at different depths with different effective closure stresses.

To upscale the findings from the lab to the field, several models have been built to predict the conductivity of propped fractures. An empirical model of fracture conductivity has been derived based on laboratory measurements on conductivity; moreover, another semi-empirical model dependent on dimensional analysis and nonlinear regression has also been developed. These two models can be used to predict conductivity in the tight gas reservoirs (Awoleke et al., 2016). A model for one-dimensional

* Corresponding authors.
E-mail addresses: zhoufj@cup.edu.cn (F. Zhou), btliang@cup.edu.cn (T. Liang).

https://doi.org/10.1016/j.egyr.2020.04.007

Table 1
Properties of 20/40 ceramic proppants and sands.

Type of proppants	Ceramic	Sand
Mesh range (mesh)	20/40	20/40
Bulk density (g/cm^3)	1.58	1.59
Apparent density (g/cm^3)	2.84	2.63
Average diameter (μm)	617	658.3
Turbidity (FTU)	14	37
Roundness (dimensionless)	0.8	0.7
Sphericity (dimensionless)	0.8	0.7
Acid-solubility (%)	6.9	7
Crushing rate (%)	5 (effective closure stress = 52 MPa)	9 (effective closure stress = 28 MPa)

suspension flow of proppant has also been put forward and verified by the laboratory tests (Keshavarz et al., 2016). Another new mathematical model has been derived to predict fracture conductivity and proppant embedment. Moreover, factors affecting the fracture conductivity have been analyzed, e.g., initial fracture aperture, the diameter of proppant, the elastic modulus of proppant and fracture wall (Li et al., 2015). Other fracture conductivity models have also been derived (Wen et al., 2005; Guo et al., 2008; Hou et al., 2016); however, these models can only describe the performance of proppants with a unique size and density, without considering their crashing with time. There is no model yet describing the performance of proppants with mixed sizes and/or materials in the propped fractures under changing effective closure stress.

In this paper, the fracture conductivity of the propped fracture with various ratios of sands to ceramic proppants is evaluated in the lab under different effective closure stresses and reservoir conditions. Based on the experimental results, two empirical models are further derived to help people to optimize the sand ratio in the slurry when hydraulically fracturing the reservoirs at different depths with different effective closure stresses.

2. Material and method

2.1. Properties of proppants

The proppants used in the experiments are ceramic proppants and sands, and their key properties are listed in Table 1. The properties showed in Table 1 were tested by the quality inspection center in the Tuha oil field (CNPC).

2.2. Experimental equipment

FCS-842, the latest Fracture Conductivity Evaluation System designed by Core Laboratories Inc., is used to conduct all conductivity tests in this study. This system can measure the fracture conductivity under maximum effective closure stress up to 138 MPa (20 000 psi) and a maximum temperature up to 177 °C (350 °F) using brine or gas, as shown in Fig. 1. The conductivity cell is designed according to ISO 13503-5.

2.3. Experimental procedure

In this study, the concentration of proppants is 5 kg/m^2 (1 lb/ft^2), which is identical to the fracturing design in the field. The temperature is 60 °C (140 °F), which is identical to the reservoir temperature. Because the fracturing fluid is at ambient temperature, the temperature in the formation would be decreased after pumped the fracturing fluid. Within each group of comparative experiments, the closure-stress increases from 10 MPa to 40 MPa with an increment of 5 MPa while all other parameters are kept the same 2 wt% KCl is used to measure the fracture conductivity,

Fig. 1. Fracture conductivity evaluation system (FCS-842).

and the testing time is 50 h for each stress point according to API RP 61 (1989). To study the change of fracture conductivity with various combinations of ceramic proppants and sands, the ratio of ceramic proppants to sands decreases from 10:0 to 0:10 among 7 comparative experiments in each group.

Fig. 2 is the schematic of the setup for measuring the fracture conductivity. The detailed procedures are presented as follows.

Step-1: A certain ratio of sands to ceramic proppant is weighed according to the experimental design.

Step-2: The proppants are placed uniformly on the bottom steel plate, which is fixed in the conductivity cell. In the field, ceramic proppants are pumped at the end of slurry injection to supports the outlet; this is simulated by putting the sands at the upstream of the cell while putting the ceramic proppants at the downstream of the cell.

Step-3: After loading the top steel plate, the conductivity cell is put into the hydraulic load frame. After upstream and downstream pipelines and 3 pressure transducers (i.e. upstream pressure, middle pressure and downstream pressure of the conductivity cell) are connected with the cell, confining pressure is applied onto the top steel plate to simulate the effective closure stress on the fracture in the reservoir.

Step-4: 2 wt% KCl is injected into the propped fracture in the conductivity cell at a certain flow rate, differential effective closure stresses are loaded according to the experimental design.

Step-5: Effective closure stresses are recorded and conductivities at each effective closure stress are calculated by Eq. (2) as below.

The permeability of the proppant pack with liquid in the state of laminar flow can be calculated by Eq. (1) from API RP 27 (1952).

$$k = \frac{99.998\mu \cdot Q_s \cdot L}{A \cdot \Delta P} \tag{1}$$

Assuming the cross-section area of the proppant pack is a perfect rectangle, the conductivity of the proppant pack can be calculated using Eq. (2) from API RP 61 (1989) and ISO 13503-5 (2006). Many researchers have used this unit to express the fracture conductivity (Gu et al., 2015; Kunnath Aven et al., 2013; Palisch et al., 2010; Pearson et al., 2014; Zhan et al., 2020). The API conductivity cell has a width of 3.8 cm and a length of 12.7 cm between two pressure ports.

$$C = \frac{5.555\mu \cdot Q_m}{\Delta P} \tag{2}$$

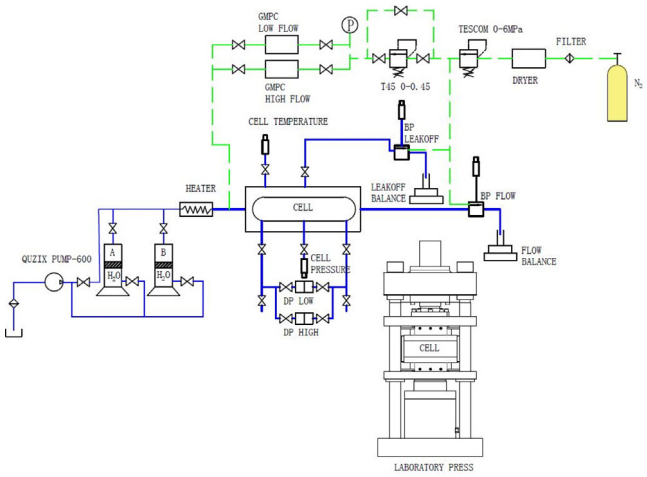

Fig. 2. Schematic of the setup for measuring the fracture conductivity.

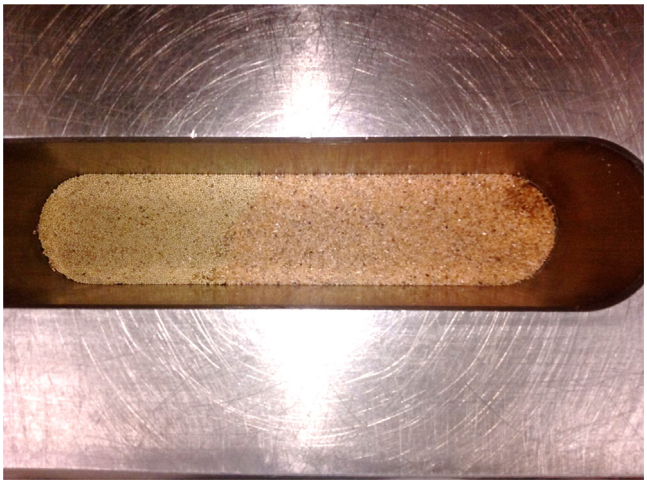

Fig. 3. Morphology of different proppants before the fracture conductivity test (Left-hand side represents the outlet and right-hand side represents inlet, ceramic to sand ratio is 4:6 in this case).

Fig. 4. Morphology of different proppants after the fracture conductivity test (Left-hand side represents the outlet and right-hand side represents the inlet, ceramic to sand ratio is 4:6 in this case).

Fig. 5. Crushing of sands near the inlet after conductivity test (ratio of ceramic proppants to sands is 4:6 in this case).

3. Results and discussion

3.1. Morphology changes of different proppants after conductivity evaluation

Figs. 3 and 4 show the morphology of different proppants within the fracture before and after the fracture conductivity test. Comparing two figures, it can be noticed that the morphology of ceramic proppants is almost unchanged, while sands have been crushed after the test.

Figs. 5 and 6 show the magnified 30 times of sands near the inlet (i.e., upstream) and ceramic proppants near the outlet (i.e., downstream) after the conductivity evaluation. It can be noticed that a large portion of sands has been pulverized (Fig. 5), which then blocks the pores and pore throats of the proppant pack. It is not observed on the ceramic proppants, only a few of which were split into halves (Fig. 6).

3.2. The conductivity of the propped fracture with various sand ratios under different effective closure stresses

Fig. 7 shows the change of fracture conductivity of the propped fracture with various ratios of ceramic proppants to sands under different effective closure stresses. As can be seen in the figure, the larger the effective closure stress, the lower the fracture conductivity, and the larger the ratio of ceramic proppants towards the outlet, the higher the fracture conductivity.

As also shown in Fig. 7, with the increasing effective closure stress, the fracture conductivities gradually decrease. The case with 100% ceramic proppants gives the highest fracture conductivity; with the increasing ratio of sands, the fracture conductivity all reduces with the effective closure stress. Under effective closure stress of 10 MPa, the conductivity of propped fracture with 100% ceramic proppants is nearly threefold to that with 100% sands. Moreover, with the increasing effective closure stress, the conductivity difference between ceramic proppants and sands is becoming larger. The conductivity of 100% sand decreases to zero under effective closure stress of 25 MPa; however, the conductivity of ceramic proppant is still as high as 150 μm^2 cm.

The proppant pack is gradually compacted with the increasing effective closure stress, which leads to a decrease of fracture width and fracture conductivity (Wen et al., 2007; Zhang et al., 2016). At small effective closure stress, higher fracture conductivity is observed in cases with more ceramic proppants, and this is attributed to the larger roundness and sphericity of ceramic proppants comparing to sands (Table 1). Large sphericity results in

Fig. 6. Crushing of ceramic proppants near the outlet after conductivity test (ratio of ceramic proppants to sands is 4:6 in this case).

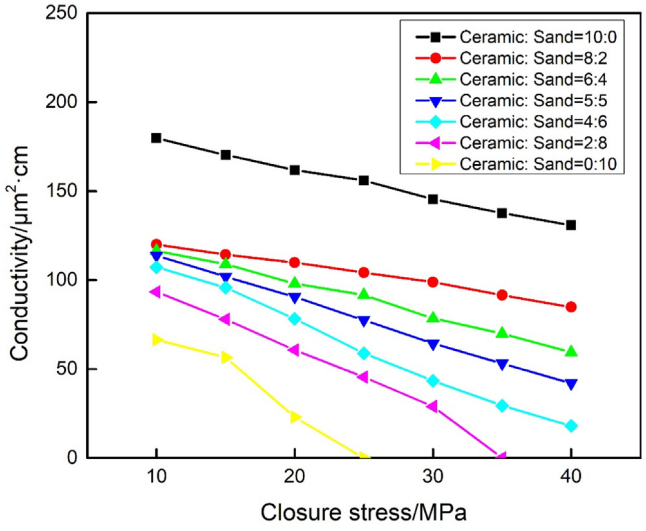

Fig. 7. Fracture conductivity of the propped fracture with various sand ratios under different effective closure stresses.

large pore space, and thus smaller flow resistance. At high effective closure stress, higher fracture conductivity is also observed in cases with more ceramic proppants, and this is attributed to the larger hardness and strength of ceramic proppants comparing to sands (Table 1). For proppants used in this work, the crushing rate of ceramic proppants under a stress of 52 MPa is 5%, while the sands under a stress of 28 MPa is 9%. In the testing environment with liquid flowing through, their difference in crushing rate is likely even larger (Palisch et al., 2010).

Fig. 7 also shows that the fracture conductivity in the case with 80% sands decreases to zero under effective closure stress of 35 MPa. Although ceramic proppants are used in this case to support the downstream of the propped fracture (i.e., outlet), fine grains of the crushed sands from the upstream can migrate with the flow downward and plug the outlet. Results indicate that using 20% of ceramic proppants can enhance the fracture conductivity by over 30%, meanwhile enhancing the tolerance of effective closure stress from 25 MPa to 35 MPa; however, it is not enough for being used in the reservoirs with effective closure stress beyond 35 MPa. Once the ratio of ceramic proppants is increased to 40%,

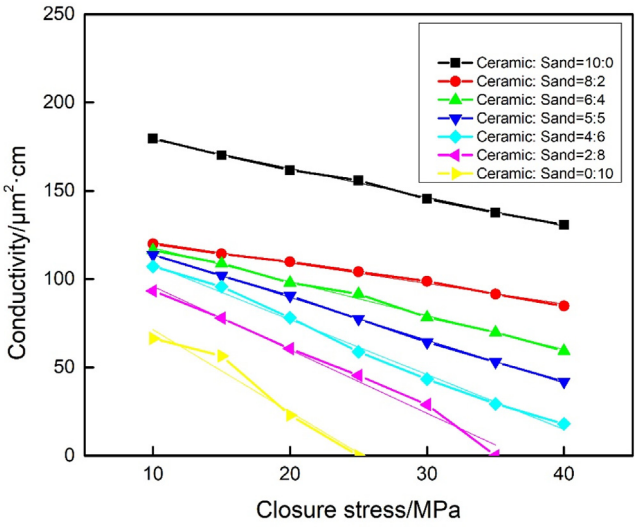

Fig. 8. Linear fit of experimental results with different sand ratios.

the fracture conductivity can remain above 20 μm^2 cm after 300 h of measurement. When more ceramic proppants are used to prop the fracture, the sands near the inlet are likely to experience less effective closure stress, and fewer fine grains are generated from the crushed sands that damage the fracture conductivity downstream. In the stage of production, the fluid pressure in the reservoir is different. The fluid pressure near the well hole is the lowest, farther distance from the well, higher fluid pressure in the reservoir. Because the effective closure stress equals to the overburden pressure minus fluid pressure, thus the effective closure stress near the well hole is the highest. Thus the ceramic with high strength was pumped in the outlet, which can bear more strength.

3.3. The relationship between the slope of conductivity with increasing effective closure stress and sand ratio

The reduction rate of fracture conductivity with the increasing effective closure stress (i.e., the slope of each conductivity curve) is calculated from linear fitting the data shown in Fig. 7, as shown in Fig. 8. All slopes of the conductivity curves are then plotted with the sand ratios of the mixed proppants in each case. Because we aim is to investigate the impact of sand with the proportion larger than zero, the combination of zero sand is not included. As shown in Fig. 9, the slope is found to be linearly proportional to the sand ratio, as described by Eq. (3). This indicates that the fracture conductivity decreases faster with the increasing effective closure stress when less sand is used. Moreover, Eq. (3) provides a convenient way to estimate the minimal needs of ceramic proppants in the slurry to keep the hydraulic fracture conductive in different reservoirs with different effective closure stress.

$$S = -0.0434P + 0.2781 \tag{3}$$

3.4. The empirical formula of fracture conductivity with the increasing effective closure stress

Based on the experimental results, an empirical formula of fracture conductivity with both the effective closure stress and the sand ratio in the mixed proppants, as listed as follows.

$$C = -(0.0434P + 0.2781)\sigma - 0.0081P^2 + 0.8078P + 118.83 \tag{4}$$

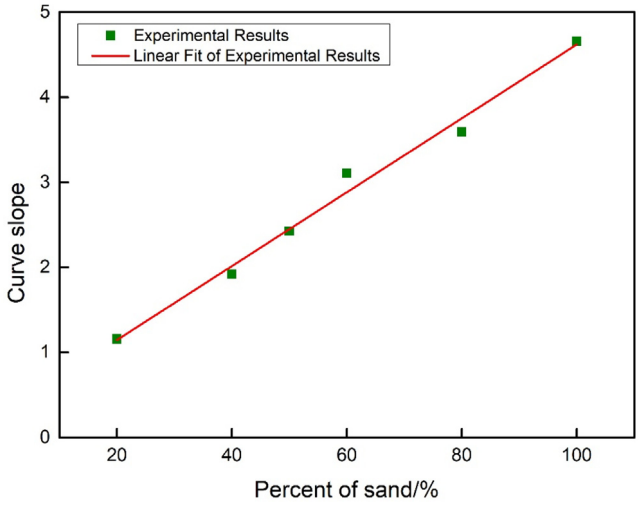

Fig. 9. Relationship between the slope of fracture conductivity with increasing effective closure stress and the sand ratio of the mixed proppants.

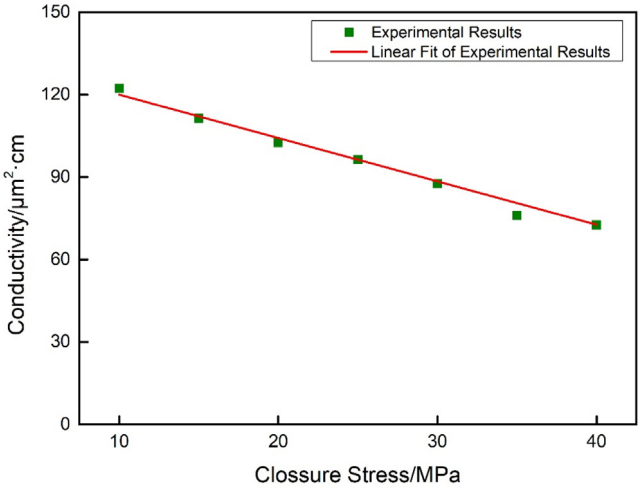

Fig. 10. Linear fit of experimental results.

It is worth mentioning that Eq. (3) is the simpler form of Eq. (4) without considering the influence of the effective closure stress. To verify the accuracy of the empirical formula, another experiment with the ratio of ceramic proppant to sand is 7:3 is conducted. As shown in Fig. 10, the new data matches well with that predicted by Eq. (4), and the error is less than 5%.

4. Conclusions

(1) With the increasing effective closure stress, the fracture conductivity gradually decreases. The highest conductivity is observed in the case with 100% ceramic proppants, while the lowest conductivity is observed in the case with 100% sands. With the increasing proportion of sand, the fracture conductivity is decreasing at all measured effective closure stresses. Observation agrees with the prediction based on the hardness and sphericity of different proppants.

(2) Under the low effective closure stress, the fracture conductivity with 100% ceramic proppants can be 3 times of that 100% sands. Moreover, with the increasing effective closure stress, the conductivity gap between cases with only ceramic proppants or sands is gradually becoming wider.

(3) According to the microscopic observation, sands tend to be crushed into small debris, while ceramic proppants tend to be crushed into big debris. Thus, the sand-propped fracture is easier to be blocked by debris, resulting in a sharply decreased fracture conductivity under the effective closure stress.

(4) An empirical formula is developed and verified by the experimental results, and it can predict fracture conductivity with the increasing effective closure stress and sand proportion. This formula can help forecast the fracture conductivity with different sand ratios and effective closure stresses for field operations.

Nomenclature

σ:	Effective closure stress, MPa
μ:	Viscosity of the fluid flowing through the proppant pack, cP
ΔP:	Pressure drop across proppant pack, kPa
A:	Area of cross section, cm^2
C:	Fracture conductivity of proppant pack, μm^2 cm
L:	Length between pressure ports on the proppant cell, cm
k:	Permeability of proppant pack, μm^2
$M_{ceramic}$:	Mass ratio of ceramic proppant, dimensionless
M_{sand}:	Mass ratio of sand, dimensionless
P:	Percentage of sand, %
Q_m:	Flow rate of the fluid through the proppant pack, cc/min
Q_s:	Flow rate of the fluid through the proppant pack, cc/s
S:	Reduction rate of fracture conductivity with the increasing effective closure stress, μm^2 cm/MPa

Declaration of competing interest

The authors declare that they have no known competing financial interests or personal relationships that could have appeared to influence the work reported in this paper.

CRediT authorship contribution statement

Xingyuan Liang: Investigation, Writing - original draft, Writing - review & editing. **Fujian Zhou:** Resources, Supervision, Funding acquisition. **Tianbo Liang:** Writing - review & editing, Methodology. **Yixiao Huang:** Visualization, Validation. **Dongya Wei:** Methodology. **Shiying Ma:** Formal analysis.

Acknowledgments

This work is financially supported by the Foundations of State Key Laboratory of Petroleum Resources and Prospecting, China (Grant Nos. PRP/indep-4-1703 and PRP/indep-4-1314), the National Science and Technology Major Projects of China (2016ZX05051 and 2017ZX05030), PetroChina Innovation Foundation, China (2018D-5007-0205), and the Science Foundation of China University of Petroleum at Beijing (Grant No. 2462017YJRC031).

References

API RP 27, 1952. Recommended practice for determining permeability of porous media third edition.

API RP 61, 1989. Recommended Practices for Evaluating Short Term Proppant Pack Conductivity. API, Washington, DC.

Awoleke, O.O., Zhu, D., et al., 2016. New propped-fracture-conductivity models for tight gas sands. SPE J. 21 (05), 1,508–1,517. http://dx.doi.org/10.2118/179743-PA, SPE-179743-PA.

Gu, M., Dao, E., Mohanty, K.K., 2015. Investigation of ultra-light weight proppant application in shale fracturing. Fuel 150, 191–201. http://dx.doi.org/10.1016/j.fuel.2015.02.019.

Guo, J., Lu, C., Zhao, J., 2008. Experimental research on proppant embedment. J. China Coal Soc. 33 (6), 661–664.

Hou, T., Zhang, S., Yu, B., et al., 2016. Theoretical analysis and experimental research of channel fracturing in unconventional reservoir. In: Presented at the SPE Europec Featured at 78th EAGE Conference and Exhibition. SPE-180105-MS, Vienna, http://dx.doi.org/10.2118/180105-MS.

Keshavarz, A., Badalyan, A., Johnson, R., et al., 2016. Productivity enhancement by stimulation of natural fractures around A hydraulic fracture using micro-sized proppant placement. J. Nat. Gas Sci. Eng. 33, 1010–1024. http://dx.doi.org/10.1016/j.jngse.2016.03.065.

Kunnath Aven, N., Weaver, J., Loghry, R., Tang, T., 2013. Long-term dynamic flow testing of proppants and effect of coatings. In: Presented at the SPE European Formation Damage Conference & Exhibition. Society of Petroleum Engineers, http://dx.doi.org/10.2118/165118-MS.

Lei, W., Shicheng, Z., Wenzong, Z., Qingzhi, W., 2005. Experimental research on long-term conductivity of the proppant combination with different grain sizes in complex fracturing. Nat. Gas Ind. 25, 64–66.

Li, K., Gao, Y., Lyu, Y., et al., 2015. New mathematical models for calculating proppant embedment and fracture conductivity. SPE J. 20 (03), 496–507. http://dx.doi.org/10.2118/155954-PA.

Liang, T., Zhou, F., Shi, Y., Liu, X., Wang, R., Li, B., Li, X., 2018. Evaluation and optimization of degradable-fiber-assisted slurry for fracturing thick and tight formation with high stress. J. Pet. Sci. Eng. 165, 81–89. http://dx.doi.org/10.1016/j.petrol.2018.02.010.

Maity, D., Ciezobka, J., 2019. An interpretation of proppant transport within the stimulated rock volume at the hydraulic-fracturing test site in the permian basin. SPE Reserv. Eval. Eng. 22, 477–491. http://dx.doi.org/10.2118/194496-PA.

Merey, Ş., 2019. Prediction of transport properties for the eastern mediterranean sea shallow sediments by pore network modelling. J. Pet. Sci. Eng. 176, 403–420. http://dx.doi.org/10.1016/j.petrol.2019.01.081.

Mittal, A., Rai, C.S., Sondergeld, C.H., 2018. Proppant-conductivity testing under simulated reservoir conditions: Impact of crushing, embedment, and diagenesis on long-term production in shales. SPE J. 23, 1,304–1,315. http://dx.doi.org/10.2118/191124-PA.

Palisch, T.T., Duenckel, R., Chapman, M.A., et al., 2010. How to use and misuse proppant crush tests: Exposing the top 10 myths. SPE Prod. Oper. 25 (03), 345–354. http://dx.doi.org/10.2118/119242-PA.

Pearson, C.M., Griffin, L., Chikaloff, J., 2014. Measuring field supplied proppant conductivity: Issues discovered in an operator. In: Presented at the SPE Hydraulic Fracturing Technology Conference. Society of Petroleum Engineers, http://dx.doi.org/10.2118/168641-MS.

Wen, Q., Zhang, S., Wang, L., et al., 2005. Influence of proppant embedment on fracture long-term flow conductivity. Nat. Gas Ind. 25 (5), 65–68.

Wen, Q., Zhang, S., Wang, L., et al., 2007. The effect of proppant embedment upon the long-term conductivity of fractures. J. Pet. Sci. Eng. 55 (3), 221–227. http://dx.doi.org/10.1016/j.petrol.2006.08.010.

Zhan, L., Tokan-Lawal, A., Fair, P., Dombrowski, R., Liu, X., Almarza, V., Girardi, A.M., Li, Z., Li, R., Pilko, M., Joost, N., 2020. Quantifying total apparent hydraulic fracture conductivity and its significant degradation from systematic bottomhole pressure measurements in permian wells. SPE Reserv. Eval. Eng. http://dx.doi.org/10.2118/201091-PA.

Zhang, J., Zhu, D., Hill, A.D., 2016. Water-induced damage to propped-fracture conductivity in shale formations. SPE Prod. Oper. 31 (02), 147–156. http://dx.doi.org/10.2118/173346-PA.

Zhang, F., Zhu, H., Zhou, H., Guo, J., Huang, B., 2017. Discrete-element-method/computational-fluid-dynamics coupling simulation of proppant embedment and fracture conductivity after hydraulic fracturing. SPE J. 22, 632–644. http://dx.doi.org/10.2118/185172-PA.

Zoveidavianpoor, M., Gharibi, A., bin Jaafar, M.Z., 2018. Experimental characterization of a new high-strength ultra-lightweight composite proppant derived from renewable resources. J. Pet. Sci. Eng. 170, 1038–1047. http://dx.doi.org/10.1016/j.petrol.2018.06.030.